Icarus 253 (2015) 149–155

Contents lists available at ScienceDirect

Icarus

journal homepage: www.elsevier.com/locate/icarus

Variations of carbon monoxide in the martian lower atmosphere

Vladimir A. Krasnopolsky *,[1]

Department of Physics, Catholic University of America, Washington, DC 20064, USA
Moscow Institute of Physics and Technology (PhysTech), Dolgoprudnyy, Russia

ARTICLE INFO

Article history:
Received 22 December 2014
Revised 5 March 2015
Accepted 5 March 2015
Available online 13 March 2015

Keywords:
Mars
Mars, atmosphere
Atmospheres, composition
Abundances, atmospheres
Spectroscopy

ABSTRACT

Our observations of variations of CO on Mars by means of the ground-based spatially-resolved high-resolution spectroscopy (Krasnopolsky, V.A. [2003]. J. Geophys. Res. 108(E2), 5010; Krasnopolsky, V.A. [2007]. Icarus 190, 93–102) have been significantly improved using the ^{13}CO lines near 4148 cm^{-1} and the CO_2 lines near 4570 cm^{-1}. These lines are of optimal strength, of low sensitivity to variations of temperature, and covered by the ATMOS solar spectrum that makes it possible to use the synthetic spectra technique for retrieval of CO and CO_2 to get CO mixing ratios. The CO_2 line strengths from Toth et al. (2008) were also essential to improve accuracy of the results.

The $^{13}CO/CO$ ratio of 1.023 times the terrestrial carbon isotope ratio was calculated using the known $^{13}CO_2/CO_2 = 1.046$ in the martian atmosphere (Webster, C.R., et al. [2013]. Science 341, 260–263), the photo-induced isotope fractionation (Miller, C.E., Yung, Y.L. [2000]. J. Geophys. Res. 105(D23), 29039–29051) in the CO_2 photolysis, and isotope fractionation in the reaction between CO and OH (Feilberg, K.L., Johnson, M.S., Nielsen, C.J. [2005]. Phys. Chem. Chem. Phys. 7, 2318–2323).

The observations were conducted at $L_S = 60°$, 89°, 110°, and 145° and extend over the maximum of CO in the southern hemisphere during the northern summer. The CO mixing ratio was observed to be constant over the 55°S–90°N latitudinal range to within 7%, for each observed L_S period. Therefore our observations show that the enrichment of incondensable gases by condensation of CO_2 in the southern polar regions does not significantly extend to the middle and low latitudes. This behavior agrees with the Mars Climate Database (Lefevre, F., Forget, F. [2009]. Nature 460, 720–722), whereas most other observations exhibit much larger latitudinal gradients and seasonal variations. Our measurements do not show the CO depletion at high northern latitudes predicted by MCD of ~20% at $L_S \approx 60–150°$ and observed as much stronger by MRO/CRISM (Toigo, A.D., et al. [2013]. J. Geophys. Res. 118E, 89–104).

The retrieved global and annually mean CO abundance is equal to 700 ppm on Mars, which is also smaller than many recent results by a factor of ~1.4.

1. Introduction

CO was detected on Mars in the first high-resolution Fourier-transform spectra (Kaplan et al., 1969), and the retrieved mixing ratio was 800 ± 300 ppm. Much later ground-based spatially resolved high-resolution spectroscopy became possible using the CSHELL spectrograph at the NASA Infrared Telescope Facility (IRTF) on Hawaii and some other instruments. Krasnopolsky (2003) observed variations of the CO mixing ratio in the lowest scale height at $L_S = 112°$ using lines of the CO (3-0) band at 1.58 μm and nearby CO_2 lines. (Solar longitude L_S determines seasons on Mars, with 0° and 180° corresponding to vernal and fall equinoxes. $L_S = 112°$ refers to a peak of the northern summer, July 14 in the terrestrial calendar.) The observed latitudinal dependence of the CO mixing ratio showed a constant value of 830 ppm from 75°N to 23°N with a linear increase to 1250 ppm at 50°S, that is, by a factor of 1.5. This increase was explained by condensation of CO_2 in the southern polar and subpolar regions that results in enrichment of incondensable gases (N_2, Ar, O_2, CO, H_2, CH_4, etc.). This new phenomenon was later confirmed in observations of Ar using the gamma-ray spectrometer onboard the Mars Odyssey orbiter (Sprague et al., 2004, 2012). Krasnopolsky (2007) continued the observations of CO at three other seasons ($L_S = 10°$, 173°, and 312°).

The Omega low-resolution imaging spectrograph at the Mars Express orbiter was applied to study seasonal variation of CO at

* Address: Department of Physics, Catholic University of America, Washington, DC 20064, USA.

[1] Visiting Astronomer at the Infrared Telescope Facility, which is operated by the University of Hawaii under Cooperative Agreement No. NCC 5-538 with the National Aeronautic and Space Administration, Science Mission Directorate, Planetary Astronomy Program.

http://dx.doi.org/10.1016/j.icarus.2015.03.006
0019-1035/

Hellas basin (Encrenaz et al., 2006) that is ~6 km deep and extends at 30–50°S and 50–80°E. Using the CO (2-0) band at 2.35 μm, mean CO was observed at 1150 ppm in the seasons of L_S = 250–360–50° and twice this value near 135°. Their LMD general circulation model showed a doubling of the incondensable species in Hellas relative to the nearby regions in northern summer. To check this prediction, Encrenaz et al. (2006) compared an observation at Hellas (40°S) with that at the north of Hellas at 23°S and confirmed the twofold difference. The observations by Krasnopolsky (2003) covered Hellas as well, and the similar difference was a factor of 1.75.

Billebaud et al. (2009) studied variations of CO using observations of the CO (1-0) band at 4.7 μm by the Planetary Fourier Spectrometer (PFS) at Mars Express. The observations covered seasons from L_S = 330° to 50°. CO at L_S = 330–360° was constant at ~1200 ppm from 40°N to 10°S decreasing to 750 ppm at 65°N. The data at L_S = 0–30° were constant at ~1100 ppm from 20°S to 30°N decreasing to 450 ppm at 60°S and 800 ppm at 50°N.

The MEX/PFS observations of the CO (2-0) band in all seasons for two and half martian years were analyzed by Sindoni et al. (2011). CO at L_S = 90–120° varies in that study from 600 ppm at 80°N to 750 ppm at 40°N, 1000 ppm at the equator, and 2000 ppm at 20°S. The variations at L_S = 240–270° are from 900 ppm at 40°N to 600 ppm at the equator and 520 ppm at 60°S.

CO on Mars is also observed using the low-resolution imaging spectrometer CRISM (Smith et al., 2009) at the Mars Reconnaissance Orbiter (MRO). The observations of the CO (2-0) band at 2.35 μm for two and half martian years were analyzed by Toigo et al. (2013). The observed latitude range varies with season from 35°S–90°N at L_S = 90° to 90°S–40°N at L_S = 270°. The observed so-called enhancement factor for CO at 30–45°S shows a linear decrease from 1.5 at L_S = 0° to 1.0 at 340° with a jump to 1.5 at 360°. A peak of 2.0 centered at L_S = 150° with a full width at half maximum of 50° overlaps this trend. Strong minima of CO in the subpolar regions of 60–90° were observed on the south at L_S = 200–300° and on the north at L_S = 60–150° with typical mixing ratios of ~200 and ~350 ppm, respectively.

Thus one may conclude that the Mars Express and MRO observations also indicate some increase in CO mixing ratio at southern latitudes in northern summer as observed by Krasnopolsky (2003). However, there are significant quantitative differences between the data from different teams and instruments.

Surprisingly, the latitudinal coverage of the spacecraft observations of CO is even smaller than that of the ground-based observations (down to 35°S and 50°S, respectively, at $L_S \approx 90°$). While the observations from the Mars orbiters have obvious advantages in spatial resolution and regularity, the much better spectral resolution in the CSHELL/IRTF observations gives some rewards as well. Therefore we continued our study of CO on Mars, and this is a subject of this paper.

2. Choice of the CO and CO_2 lines

While the orbiter studies of CO on Mars are mostly based on the CO (2-0) band at 4260 cm^{-1}, our retrievals in Krasnopolsky (2003, 2007) involved the lines R12 6390.82 cm^{-1} and R13 6393.18 cm^{-1} of the CO (3-0) band. A blend of four lines at 6380.85–6381.18 cm^{-1} was used for the CO_2 retrieval.

Both CO and CO_2 lines were observed in the same spectra by Krasnopolsky (2003, 2007), and that was beneficial for the derived CO mixing ratios. However, solar high-resolution spacecraft spectra are lacking for ν > 4800 cm^{-1}; therefore it was impossible to apply the synthetic spectra technique to extract the CO and CO_2 abundances. We used the equivalent width tools for this purpose, whose accuracy is lower. Furthermore, CO lines are significant in the solar spectrum, their Doppler shift from the martian CO lines is small because of the low heliocentric velocity of Mars, and careful corrections for those lines require spacecraft solar spectra. These spectra were measured up to 4800 and 4400 cm^{-1} with resolution 0.01 and 0.02 cm^{-1} by the ATMOS (Farmer and Norton, 1989) and ACE (Hase et al., 2010) orbiters, respectively. We will apply a version of the ATMOS spectrum suggested by Kurucz (2011, http://kurucz.harvard.edu/sun/atmos/).

Therefore we choose the CO (2-0) band to utilize the synthetic spectra technique and to properly correct the data for the solar CO and other lines. Lines of this band that are the best for our task should (1) be not strongly contaminated by other telluric and martian lines, (2) be near the band origin, that is, have low rotational quantum numbers J, and (3) have proper strengths. While (1) is clear, (2) and (3) need some explanation.

Line strength is proportional to $\exp(-\alpha E_0/T)$; here α = 1.439 cm K, $E_0 = B_0\,J\,(J+1)$ is the lower state energy, and B_0 is the rotational constant of the lower state. If this energy is high, then the line strength strongly depends on temperature, and errors in temperature are converted in significant errors of the retrieved CO abundances.

Line equivalent width is proportional to the absorber abundance, if optical depth in the line center τ_0 is less than one. The equivalent width is weakly sensitive to the absorber abundance for $\tau_0 \gg 1$, and the best case for accurate measurements is $\tau_0 \approx 1.5$. Optical depth in the line center is

$$\tau_0 = \frac{\mu f N S}{\pi^{1/2}\Delta\nu_D}; \quad \Delta\nu_D = 4.3\times10^{-7}\nu(T/m)^{1/2}.$$

Here $\mu \approx 3$ is the two-way airmass, f is the species mixing ratio (~10^{-3} for CO), $N \approx 2.3\times10^{23}$ cm^{-2} is the column number of molecules on Mars, S is the line strength, $\Delta\nu_D$ is the Doppler line width, ν is the wavenumber, and m is the molecular mass in the atomic units. Then the best case is $S \approx 3\times10^{-23}$ cm for CO and ~3×10^{-26} cm for CO_2.

Choosing the lines for the CO observations, one should bear in mind a very small spectral coverage of CSHELL for a chosen grating position. This coverage is 0.0023 ν_0, and ν_0 is a chosen central wavenumber.

Requirements (2) and (3) look contradictory for the CO (2-0) band, because the lines with low J have strengths exceeding our preferable value by two orders of magnitude. The contradiction is removed if lines of the ^{13}CO isotopologue are used. We choose the ^{13}CO (2-0) lines P6 4143.787 cm^{-1}, P5 4147.788 cm^{-1}, and P4 4151.724 cm^{-1}. Their E_0 are 77, 55, and 37 cm^{-1}, and their strengths are 3.6, 3.5, and 3.2 times 10^{-23} cm, respectively, at T = 200 K. The chosen lines fit all our criteria.

The similar requirements are applied to the CO_2 lines for our observations. We choose seven lines of the CO_2 (31103-00001) band between P32e 4565.849 cm^{-1} and P20e 4575.396 cm^{-1}. Their E_0 vary from 412 to 164 cm^{-1}, their strengths from 2.3 to 2.9 times 10^{-26} cm at 200 K.

Products $f\,S$ are similar for the chosen lines of CO and CO_2, their equivalent width are expected to be similar as well, and some error in their extraction may cancel out in their ratios.

The spectroscopic database HITRAN 2012 (Rothman et al., 2013) gives uncertainties of the chosen line strengths as 2–5% for the ^{13}CO lines and >20% for the CO_2 lines. The most accurate data for the CO_2 lines were measured by Toth et al. (2008), and those data had not been included in HITRAN 2012. Differences between the line strengths of our interest in Toth et al. (2008) and HITRAN 2012 are ~2.5%, and we will use the data from Toth et al. (2008) with a good confidence.

The chosen lines look significantly better for our task than those in Krasnopolsky (2003, 2007). However, now the CO and CO_2 lines are not observed simultaneously but with an interval of ~15 min.

Mars rotates 14.6 degrees per hour, and the shift between the CO and CO_2 observations is 3.7°, that is, a third of the instrument spatial resolution near the equator. This shift is neither significant nor negligible, and we cannot compensate it in the retrieved CO mixing ratios.

3. $^{13}CO/^{12}CO$ in the martian atmosphere

We have to involve a ratio of $^{13}CO/^{12}CO$ in interpretation of our observations of variations of the CO mixing ratio in the martian atmosphere. We have not found this ratio in the literature and will calculate it here.

Both the tunable laser spectrometer and the quadrupole mass spectrometer at the Curiosity rover (Webster et al., 2013; Mahaffy et al., 2013) observed $^{13}CO_2/^{12}CO_2 = 1.046$ times the terrestrial ratio of $^{13}C/^{12}C = 0.011235$. Balance of ^{13}CO in Mars' atmosphere is determined by reactions

$$^{13}CO_2 + h\nu \rightarrow {}^{13}CO + O$$
$$^{13}CO + OH \rightarrow {}^{13}CO_2 + H.$$

Rate coefficients of these reactions may differ from those for the basic isotopologues. The rate of the $^{13}CO_2$ photolysis is generally unknown; however, there are simple means to evaluate it.

Photo-induced isotope fractionation was considered by Miller and Yung (2000). They argued that photolysis cross sections of isotopologues are similar with a small shift in the energy scale that is equal to difference in zero point energies (ZPE). Miller and Yung (2000) did not define this term and just mentioned that ZPEs may be calculated "using experimentally measured vibrational frequencies".

Vibrational term of a molecule is

$$G(v) = \omega_e(v+1/2) - \omega_e x_e(v+1/2)^2 + \omega_e y_e(v+1/2)^3$$

Here v is the vibrational quantum number, ω_e is the vibrational frequency, and x_e and y_e are small corrections for unharmonicity. The CO_2 molecule has three vibration modes (symmetric, bending, and antisymmetric), and we believe that its ZPE is sum of three vibrational terms for $v = 0$. We will neglect the corrections for unharmonicity and calculate ZPE for CO_2 and $^{13}CO_2$ using HITRAN. There is no change in dipole moment for the symmetric mode, and it is strongly forbidden. Therefore we use the band (11101-00001), which gives a sum of the symmetric and bending modes, and then the antisymmetric band (00011-00001). The calculated difference in ZPE between CO_2 and $^{13}CO_2$ is 53 cm^{-1}.

The solar spectrum at 180–210 nm is proportional to $e^{0.095\lambda(nm)}$ (Fig. 1). The shift by 53 cm^{-1} is equal to 0.212 nm at 200 nm and results in reduction in the $^{13}CO_2$ photolysis rate by a factor of $e^{0.095*0.212} = 1.020$.

The reaction between various CO isotopologues and OH was studied by Feilberg et al. (2005). Unfortunately, a ratio of the rate coefficients for $^{13}C^{16}O/^{12}C^{16}O$ was not measured. We assume the following rate ratio:

$$^{12}C^{16}O/^{12}C^{18}O = {}^{13}C^{16}O/^{13}C^{18}O = 0.977 \pm 0.005.$$

Then the rate ratio is

$$^{13}C^{16}O/^{12}C^{16}O = \frac{^{13}C^{16}O/^{12}C^{18}O}{^{12}C^{16}O/^{12}C^{18}O} = \frac{0.979 \pm 0.005}{0.977 \pm 0.005} = 1.002 \pm 0.007.$$

The numerical data are from Feilberg et al. (2005). Therefore the abundance ratio is

$$^{13}CO/CO = 1.046/1.020/1.002 = 1.023$$

times the terrestrial carbon isotope ratio. We will correct our retrievals for this factor. In any case, $^{13}CO/CO$ is close to the terrestrial carbon isotope ratio, and we may use the ^{13}CO lines with a great confidence.

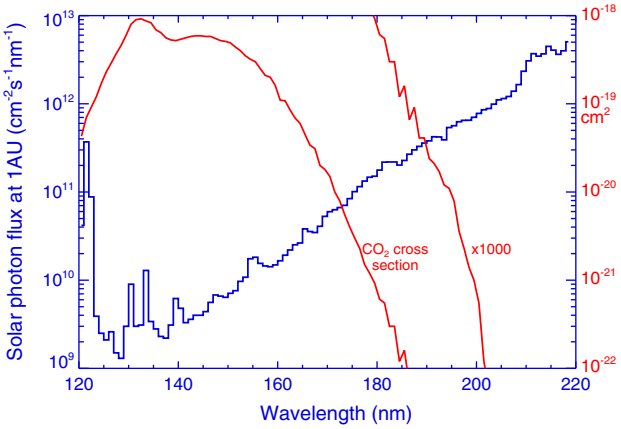

Fig. 1. Solar spectrum at 120–220 nm (Woods et al., 1996) and CO_2 absorption cross section at 195 K (Parkinson et al., 2003). The right red curve is the CO_2 cross section at 184–202 nm scaled by a factor of 1000. (For interpretation of the references to colour in this figure legend, the reader is referred to the web version of this article.)

Vibrational frequencies are proportional to $\mu^{-1/2}$; here μ is the reduced mass and

$$\frac{1}{\mu} = \frac{1}{m_0} + \frac{1}{m_1}$$

where m_0 and m_1 are masses of atoms in a molecule. Therefore vibrational frequencies related to deuterium in hydrides are smaller than those for hydrogen by factors of 1.3–1.4. This induces significant differences in ZPEs and photolysis rates (by a factor of 2.5 for HDO relative to H_2O on Mars (Miller and Yung, 2000)). Therefore photo-induced isotope fractionation may be very significant for hydrides and typically much smaller for other species.

4. Observations

We used the long-slit high-resolution spectrograph CSHELL (Greene et al., 1993) at NASA IRTF. The spectrograph selects a narrow spectral interval of 0.0023 ν_0, and the central wavenumber ν_0 may be chosen in the wide range of 1800–9000 cm^{-1} (5.6–1.08 μm). The instrument detector is an InSb array of 256 × 150 pixels cooled to 30 K. Each pixel is 9×10^{-6} ν_0 in the dispersion direction and 0.2 arcs in the aspect direction. The instrument resolving power is $\nu/\delta\nu = 40{,}000$. The telescope diameter is 3 m, and its position on the summit of Mauna Kea (Hawaii) with elevation of 4.2 km, mean overhead water of 2 pr. mm, pressure of 0.6 bar, and perfect astroclimate is favorable for high-resolution spectroscopy of the planetary atmospheres. Total spatial resolution of the telescope and spectrograph is ~1 arcs.

We had four sessions to observe variations of CO on Mars using the combination of the ^{13}CO lines near 4148 cm^{-1} and the CO_2 lines near 4570 cm^{-1}. Summary of the observing conditions is in Table 1. The instrument slit was directed along the central meridian of Mars (Fig. 2), and the observations involved exposures of Mars, sky foreground 30 arcs off Mars, flat field from a continuum source, dark current, and a nearby star for focusing.

Dates of the observations were chosen to get reasonable combinations of the Mars angular size and geocentric velocity that determines the Doppler shift. The CO and CO_2 abundances on Mars exceed those on the Earth by orders of magnitude, and a large Doppler shift is not very important for our task. However, we combined a few tasks in our observations, and the Doppler shift was

Table 1
Observing conditions in four sessions for ^{13}CO 4148 cm^{-1} and CO_2 4570 cm^{-1}.

Dates	2012-01-22	2012-05-11	2014-02-12	2014-06-03
L_S	60°	110°	89°	145°
Angular diameter (arcs)	10.9	9.2	9.9	11.6
Local time	14:00	9:20	14:16	9:35
Subearth latitude	23°	24°	20°	25°
Subsolar latitude	22°	24°	25°	16°
Longitude	70°W	116°W	75°W	68°W
Geocentric velocity (km/s)	−13.4	13.9	−15.7	10.9
Heliocentric velocity (km/s)	0.4	−1.4	−0.7	−2.1
Phase (Sun–Mars–Earth) angle	27.5°	36.4°	31.8°	35.1°

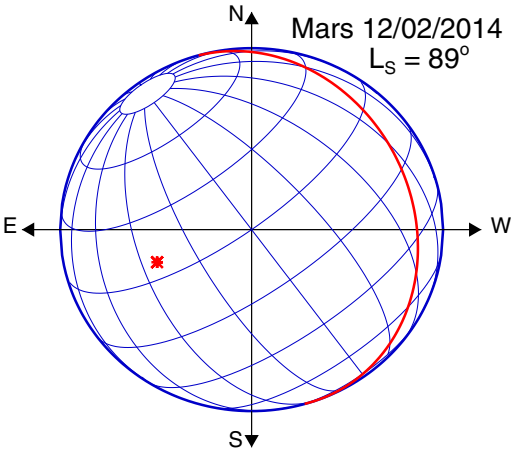

Fig. 2. Mars in the celestial coordinates as seen on February 12, 2014. The subsolar point and terminator are shown in red. The central meridian is at 75°W. Observations along the central meridian extend from 50°S to 90°N. (For interpretation of the references to colour in this figure legend, the reader is referred to the web version of this article.)

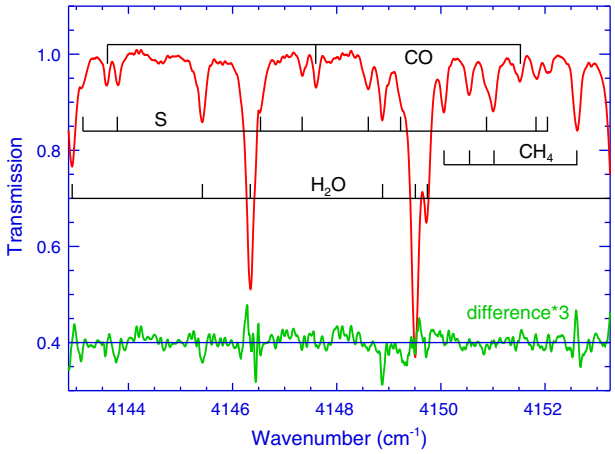

Fig. 3. Spectrum at 4143–4153 cm^{-1} observed at the subsolar latitude of 24°N at L_S = 110°. All absorption lines are identified; the solar lines are marked S. Difference between the observed and synthetic spectra is shown scaled by a factor of 3.

critical for some of them. Then the optimal dates are two months before and after the Mars opposition.

5. Data processing and analysis

As in our previous observations using CSHELL/IRTF, differences between the martian spectra and those of the sky foreground are divided by differences between the flat field spectra and the dark current. This operation results in corrections for foreground, flat field, and dark current. Then we search for bad pixels and replace them by mean values of their two neighbors.

We do not account for aerosol scattering in our analysis. Aerosol slightly reduces apparent abundances of species in spectroscopic observations of the martian atmosphere. This reduction is rather similar for CO and CO_2, which are measured at close wavenumbers, and compensated in the CO/CO_2 ratios.

Our technique for fitting the observed spectra by synthetic spectra requires conversion of the observed spectra to a wavenumber scale with a step of 0.001 cm^{-1}. We apply for this purpose a parabolic fitting of three adjacent pixels that transforms a pixel value to eight sampling points and keeps the sum of these points at the pixel value. (This is better for our analysis than the standard parabolic fitting that fixes the middle sampling point at the pixel value.) Then wavenumber scales are determined using identified lines in the spectra, and the spectra are linearly interpolated to the step of 0.001 cm^{-1}.

Both the instrument sensitivity and the martian reflectivity may slightly vary with wavenumber within a spectrum, and we use a parabola (three parameters) to compensate for these variations. Optical interactions between some parts of the instrument make a weak sinusoidal component in the spectrum that is subtracted using three parameters (amplitude, period, and phase). This sinusoidal has a period exceeding the resolution element by a factor of ∼15 and amplitude of ∼1%. Its subtraction helps getting a more accurate fitting of the spectral continuum. Small errors in wavenumbers result in significant differences between the observed and synthetic spectra. Therefore we apply wavenumber corrections at the edges and in the middle of the observed spectrum. Overall, nine parameters are used to adjust each observed spectrum.

A typical angular diameter of Mars is 10 arcs in our observations, the pixel size is 0.2 arcs, and we have 50 spectra along the central meridian. A processed spectrum of CO observed at the subsolar latitude of 24°N on May 2012 (L_S = 110°) is shown in Fig. 3. All significant absorption lines are identified in the figure. Except the CO lines, there are strong solar lines and telluric lines of H_2O and CH_4.

Synthetic spectra are based on the solar high-resolution ATMOS spectrum (see Section 2) that is Doppler-shifted by a sum of geocentric and heliocentric velocities of Mars (Table 1). Telluric water is approximated by its abundance, mean temperature and pressure. Two parameters, abundance and temperature, are used for telluric methane, and its mean pressure is equal to half the pressure of 0.6 bar at Mauna Kea. We find that the Voigt line shape gives results for the telluric H_2O and CH_4 lines that are rather similar to those for the collisional broadening, and use the latter.

The martian CO lines are calculated using the Voigt line shape and CO line broadening by CO_2 from Sung and Varanasi (2005). Half surface pressures and temperatures at these levels are required for these calculations, and the data were taken from the

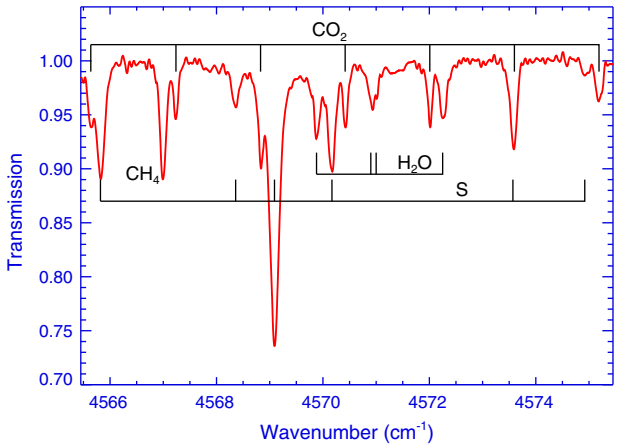

Fig. 4. Spectrum at 4565–4576 cm^{-1} observed at 24°N in May 2012 (L_S = 110°). All absorption lines are identified; the solar lines are marked S.

MGS/TES (Smith, 2004) for proper seasons, latitudes, and longitudes at three martian years and averaged. One more parameter is the instrument spectral resolution that is approximated by a Gaussian with a variable width. Overall we have nine parameters to adjust the observed spectrum and seven parameters to calculate the synthetic spectrum. The number of free parameters is much smaller than the number of degrees of freedom (256 pixels in a spectrum). The synthetic spectrum that fits the observed spectrum in Fig. 3 is not shown, because both spectra are very similar with a mean deviation of 0.6%. Their difference is shown scaled by a factor of 3.

The CO_2 spectra at 4565–4576 cm^{-1} are processed similarly. The spectra (Fig. 4) include seven martian CO_2 lines, solar lines, and telluric H_2O and CH_4 absorption lines. All significant lines are identified in Fig. 4.

6. Results and discussion

Retrieved column CO and CO_2 abundances times airmass m for the session on May 11, 2012, are shown in Fig. 5. Both curves demonstrate strong limb brightening that disappears in their ratios that are corrected for the presence of N_2 and Ar and then for $^{13}CO/CO = 1.023$ to give the CO mixing ratios. They are rather constant with a mean value of 747 ppm and standard deviation of 42 ppm.

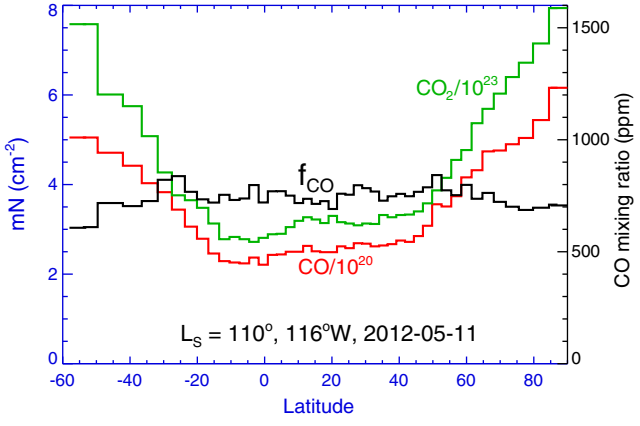

Fig. 5. Retrieved products of CO and CO_2 column abundances and airmass factors in the observation on May 11, 2012. Their ratios corrected for the presence of N_2, Ar, and for $^{13}CO/CO$ give the CO mixing ratios.

The retrieved latitudinal variations of the CO mixing ratio at four seasons in the martian lower atmosphere are shown in Fig. 6. While the seasons cover a quarter of the martian year, they encompass the peak of the expected CO variations in the southern hemisphere during the northern summer. To our great surprise, the improved observations reveal the lack of significant latitudinal variations of CO from the north pole down to 50°S in the northern summer. All four observing sessions show the flat latitudinal distributions of the CO mixing ratio.

Mean observed CO mixing ratios for all seasonal points are given in Table 2. Their standard deviations are actually sums of the CO variations and the observational random uncertainties. The mean deviation is 6.6% indicating that both values are low. The third line in Table 2 shows relative variations of atmospheric pressure taken from the Viking 1 observations (Hess et al., 1980). The CO chemical lifetime is a few years, and seasonal variations of the mean CO mixing ratio may just reflect the variations of CO_2 with the same total CO amount. Then products of the mean CO and the relative pressure P/P_0 should be constant and give the annually-mean CO abundance (Table 2). These values are equal to 681 ± 13 ppm for L_S = 60, 89, and 110°; however, the value for L_S = 145° is greater by 20%. All data were observed and analyzed similarly, and we do not have a good explanation for this difference that significantly exceeds the observational uncertainties. The mean for the values in the last line in Table 2 is 716 ± 34 ppm, and the mean CO abundance of 700 ppm may be recommended from our observational data.

The observed latitudinal dependence of the CO mixing ratio at L_S = 110° and 116°W is compared in Fig. 7 with the observations by Krasnopolsky (2003), the MEX/PFS data by Sindoni et al. (2011), and the MRO/CRISM observations (Toigo et al., 2013) at the same season. The data in Krasnopolsky (2003) at L_S = 112° are centered at 60°E and cover the deepest Hellas basin. The PFS results are zonally-mean at L_S = 90–120°. The CRISM observations are also zonally-mean for Mars year 30, and we apply approximate conversion of their color code. Predictions of the Mars Climate Database (MCD, http://wwwmars.lmd.jussieu.fr/mcd_python/) are also shown for longitudes of 60°E (including Hellas) and 116°W, similar to that in this work. The MCD is based on the LMD general circulation model with inclusion of photochemistry (Lefevre and Forget, 2009).

All data in Fig. 7 are in reasonable agreement from the equator to 30°N, where CO is almost constant with a mean value of ~700 ppm. The differences in the southern hemisphere are significant. Hellas was heavily weighted in the results by Krasnopolsky (2003). According to Encrenaz et al. (2006), the increase in CO over Hellas in northern summer is a factor of 2, and the contrast between CO at 40°S on Hellas and that at 23°S is also a factor of 2 at this season; this contrast was a factor of 1.75 in Krasnopolsky (2003). This may partly explain the observed southward increase in CO in Krasnopolsky (2003). Strong poleward temperature gradients and high sensitivity of the chosen CO_2 lines to temperature might affect the retrieved CO mixing ratios in Krasnopolsky (2003, 2007) as well. The steep increase by a factor of 2.5 from 0° to 20°S in the CO observations by MEX/PFS looks unexpected and is not supported by the other data.

The MRO/CRISM observations (Toigo et al., 2013) indicate strong depletions in CO at high latitudes of 60–90° near summer solstices. The CO mixing ratio is ~200 ppm in the southern subpolar regions at $L_S \approx$ 200–300° and ~350 ppm in the northern subpolar regions at $L_S \approx$ 60–150°. The CRISM data in Fig. 7 reflect this depletion as well. A similar depletion is predicted by MCD, though it is significantly weaker, from ~700 ppm in the middle latitudes to ~580 ppm near the north pole in Fig. 7. A weak decrease to the north pole is seen in the PFS data (Fig. 7). However, our observations for four seasons in Fig. 6 do not reveal any substantial

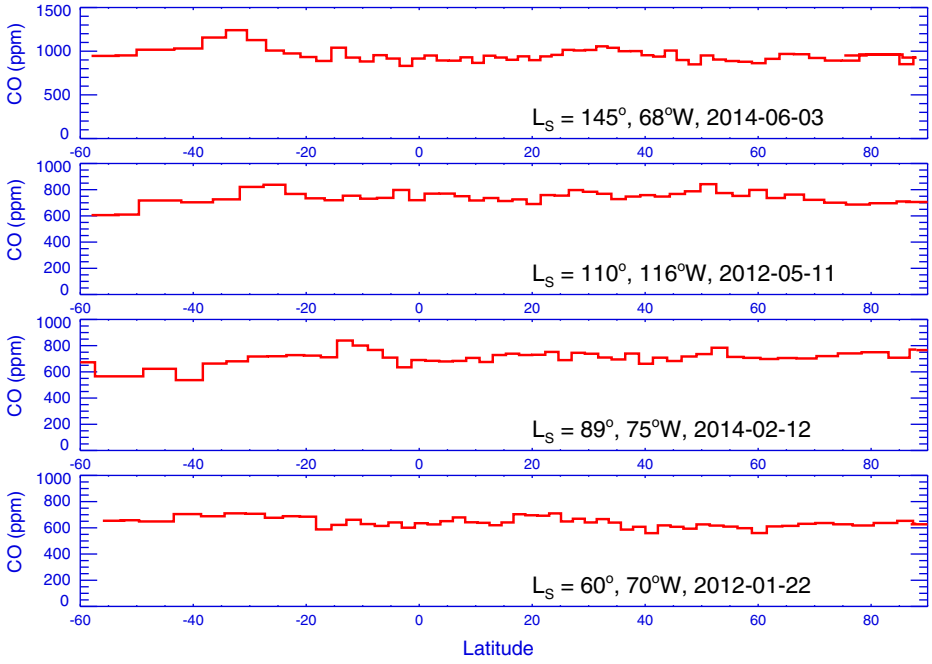

Fig. 6. Latitudinal variations of CO mixing ratio from our observations at four seasons near the expected summer maximum.

Table 2
Mean CO abundances, their variations, variations of pressure, and corrected annually mean CO abundances.

L_S	60°	89°	110°	145°
Mean CO (ppm)	641	708	747	953
Variability[a] (ppm)	37	50	42	74
P/P_0[b]	1.04	0.98	0.92	0.86
CO × P/P_0 (ppm)	667	693	684	817

[a] Standard deviations reflect variabilities here.
[b] From the Viking 1 observations (Hess et al., 1980); P_0 is the annually mean pressure.

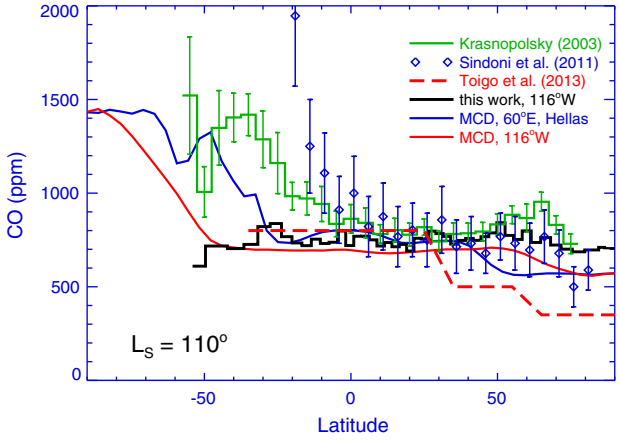

Fig. 7. Comparison of the observational and model data on latitudinal variations of the CO mixing ratio at L_S = 110°. The Mars Climate Database predictions are shown for two longitudes.

reduction in CO to the north pole. Otherwise the MCD prediction for 116°W perfectly agrees with our observation at this longitude and season.

Our observations at four seasonal points, which characterize the maximal effect of enrichment of incondensable gases by condensation of CO_2 in the southern polar regions, show that this effect does not significantly extend to the middle and low latitudes, in accord with the MCD predictions.

The global and annually mean CO mixing ratio of 700 ppm from our observations is smaller than ~1000 ppm from Krasnopolsky (2007), Billebaud et al. (2009), Hartogh et al. (2010), and Sindoni et al. (2011); an upper limit of 1000 ppm was observed by the quadrupole mass spectrometer at the Curiosity rover (Mahaffy et al., 2013).

Kaplan et al. (1969) compared P6 lines of the CO (3-0) and (2-0) bands in their first detection of CO on Mars, and the retrieved CO mixing ratio was 800 ± 300 ppm. Krasnopolsky (2007) pointed out that the CO (3-0) P6 line at 6325.80 cm^{-1} is contaminated by the CO_2 line at 6325.77 cm^{-1}. This means that a true CO mixing ratio may be smaller than that claimed by Kaplan et al. (1969). Clancy et al. (1996) observed a CO abundance of 800 ± 100 ppm using the CO and ^{13}CO lines in the millimeter range.

MCD gives the mean CO abundance of 700 ppm; however, MCD and some other general circulation models may simulate variations of long-living species but cannot predict their total abundance. For example, the lifetime of H_2 is 300 years on Mars (Krasnopolsky, 2010), and GCM simulations for a period of ~1000 years are currently technically impossible. Therefore the total CO abundance of 700 ppm was just adopted as an initial datum in the MCD.

7. Conclusions

Our observations of variations of CO on Mars by means of the ground-based spatially-resolved high-resolution spectroscopy have been significantly improved using the ^{13}CO lines near 4148 cm^{-1} and the CO_2 lines near 4570 cm^{-1}. These lines are of optimal strength, low sensitive to variations of temperature, and covered by the ATMOS solar spectrum that makes it possible to use the synthetic spectra technique for retrieval of CO and CO_2 to get CO mixing ratios. The CO_2 line strengths from Toth et al. (2008) were also essential to improve the accuracy of the results.

The $^{13}CO/CO$ ratio of 1.023 times the terrestrial carbon isotope ratio was calculated using the known $^{13}CO_2/CO_2$ = 1.046 in the

martian atmosphere (Webster et al., 2013), the photo-induced isotope fractionation (Miller and Yung, 2000) in the CO_2 photolysis, and isotope fractionation in the reaction between CO and OH (Feilberg et al., 2005).

The observations were conducted at $L_S = 60°$, 89°, 110°, and 145° and encompass the maximum of CO in the southern hemisphere during the northern summer. The observed CO extends from 55°S to the north pole. The CO mixing ratio was constant within all latitude range and for all observed seasonal points. Typical variations of CO are smaller than 7%. The results show that the enhancement of incondensable species by condensation of CO_2 in the southern polar regions at $L_S = 80–150°$ does not cover the middle and lower latitudes. This agrees with the predictions of the Mars Climate Database (Lefevre and Forget, 2009) but does not support some observations that show significant increases in CO even at low southern latitudes.

Our measurements do not show the CO depletion at high northern latitudes predicted by MCD of ~20% at $L_S \approx 60–150°$ and observed as much stronger in the MRO/CRISM observations (Toigo et al., 2013).

The retrieved global and annually mean CO abundance is equal to 700 ppm on Mars. It is smaller than those in some recent observations.

Acknowledgments

This work is supported by NASA Planetary Astronomy Program (Grant NNX12AG28G to V.A. Krasnopolsky) and by Grant 11.G34.31.0074 of the Russian Government to Moscow Institute of Physics and Technology (PhysTech) and V.A. Krasnopolsky. The author is grateful to the IRTF staff and Dave Griep, Eric Volquardsen, and Tony Matulonis, the telescope operators.

References

Billebaud, F. et al., 2009. Observations of CO in the atmosphere of Mars with PFS onboard Mars Express. Planet. Space Sci. 57, 1446–1457.
Clancy, R.T. et al., 1996. Water vapor saturation at low altitudes around Mars: A key to Mars climate? Icarus 122, 36–62.
Encrenaz, Th. et al., 2006. Seasonal variations of the martian CO over Hellas as observed by OMEGA/Mars Express. Astron. Astrophys. 459, 265–270.
Farmer, C.B., Norton, R.H., 1989. A High-Resolution Atlas of the Infrared Spectrum of the Sun and the Earth Atmosphere from Space. 1. The Sun. NASA Ref. Publication 1224, vol. 1.
Feilberg, K.L., Johnson, M.S., Nielsen, C.J., 2005. Relative rates of reaction of $^{13}C^{16}O$, $^{12}C^{18}O$, $^{12}C^{17}O$ and $^{13}C^{18}O$ with OH and OD radicals. Phys. Chem. Chem. Phys. 7, 2318–2323.
Greene, T.P. et al., 1993. CSHELL: A high spectral resolution echelle spectrograph for the IRTF. Proc. SPIE 1946, 313–323.
Hartogh, P. et al., 2010. First results on martian carbon monoxide from Hershel/HIFI observations. Astron. Astrophys. 521, L48 (5pp.).
Hess, S.L. et al., 1980. The annual cycle of pressure on Mars measured by Viking Landers 1 and 2. Geop-hys. Res. Lett. 7, 197–200.
Hase, F. et al., 2010. The ACE-FTS atlas of the infrared solar spectrum. J. Quant. Spec. Rad. Trans. 111, 521–528.
Kaplan, L.D., Connes, J., Connes, P., 1969. Carbon monoxide in the martian atmosphere. Astrophys. J. 157, L187–L192.
Krasnopolsky, V.A., 2003. Spectroscopic mapping of Mars CO mixing ratio: Detection of north-south asymmetry. J. Geophys. Res. 108 (E2), 5010.
Krasnopolsky, V.A., 2007. Long-term spectroscopic observations of Mars using IRTF/CSHELL: Mapping of O_2 dayglow, CO, and search for CH_4. Icarus 190, 93–102.
Krasnopolsky, V.A., 2010. Solar activity variations of thermospheric temperatures on Mars and a problem of CO in the lower atmosphere. Icarus 207, 638–647.
Kurucz, R.L., 2011. http://kurucz.harvard.edu/sun/atmos/.
Lefevre, F., Forget, F., 2009. Observed variations of methane on Mars unexplained by known atmospheric chemistry and physics. Nature 460, 720–722.
Mahaffy, P.R. et al., 2013. Abundance and isotopic composition of gases in the martian atmosphere from the Curiosity rover. Science 341, 263–266.
Miller, C.E., Yung, Y.L., 2000. Photo-induced isotopic fractionation. J. Geophys. Res. 105 (D23), 29039–29051.
Parkinson, W.H., Rufus, J., Yoshino, K., 2003. Absolute absorption cross section measurements of CO_2 in the wavelength region 163–200 nm and the temperature dependence. Chem. Phys. 290, 251–256.
Rothman, L.S. et al., 2013. The HITRAN 2012 molecular spectroscopic database. J. Quant. Spec. Rad. Trans. 130, 4–50.
Sindoni, G., Formisano, V., Geminale, A., 2011. Observations of water vapour and carbon monoxide in the martian atmosphere with the SWC of PFS/MEX. Planet. Space Sci. 59, 149–162.
Smith, M.D., 2004. Interannual variability in TES atmospheric observations of Mars during 1999–2003. Icarus 167, 148–165.
Smith, M.D. et al., 2009. Compact Reconnaissance Imaging Spectrometer observations of water vapor and carbon monoxide. J. Geophys. Res. 114, E00D03.
Sprague, A.L. et al., 2004. Mars' south polar Ar enhancement: A tracer for south polar seasonal meridional mixing. Science 306, 1364–1367.
Sprague, A.L. et al., 2012. Interannual similarity and variation in seasonal circulation of Mars' atmospheric Ar as seen by the gamma ray spectrometer on Mars Odyssey. J. Geophys. Res. 117, E04005.
Sung, K., Varanasi, P., 2005. CO_2-broadened half-widths and CO_2-induced line shifts of $^{12}C^{16}O$ relevant to the atmospheric spectra of Venus and Mars. J. Quant. Spec. Rad. Trans. 91, 319–332.
Toigo, A.D. et al., 2013. High spatial and temporal resolution sampling of martian gas abundances from CRISM spectra. J. Geophys. Res. 118E, 89–104.
Toth, R.A. et al., 2008. Spectroscopic database of CO_2 line parameters: 4300–7000 cm^{-1}. J. Quan. Spec. Rad. Tran. 109, 906–921.
Webster, C.R. et al., 2013. Isotope ratios of H, C, and O in CO_2 and H_2O of the martian atmosphere. Science 341, 260–263.
Woods, T.N. et al., 1996. Validation of the UARS solar ultraviolet irradiances: Comparison with the ATLAS 1 and 2 measurements. J. Geophys. Res. 101, 9541–9569.